

RESPONSE OF MULTILAYERED COMPOSITE LAMINATES TO DYNAMIC SURFACE LOADS

Shyh-Shiuh Lih

Jet Propulsion Laboratory
California Institute of Technology
Pasadena, CA 91109-8099, U.S.A.

Ajit K. Mal

Mechanical, Aerospace and Nuclear Engineering Department
University of California, Los Angeles
Los Angeles, CA 90095 - 1597, U.S.A.

ABSTRACT

A theoretical investigation of the response of multilayered composite laminates to concentrated and distributed dynamic surface loads is carried out. Each layer of the laminate is assumed to be transversely isotropic and dissipative with arbitrarily y oriented symmetry axis. The dissipative property of the material is modeled approximately through the introduction of a frequency dependent damping function. A multiple transform technique is used to calculate the spectra and time histories of the displacements and stresses produced by a variety of dynamic loads, and the quantitative features of the waves produced in the laminate are determined. The methodology developed in this work is expected to be useful in the prediction of the response of composite laminates to impact loads and also in the characterization of acoustic emission (AE) sources in these materials under static and dynamic loads.

I. INTRODUCTION

It is well known that laminated composites often suffer significant internal damage when they are subjected to localized dynamic surface loads. The damage may involve fiber breakage and debonding as well as delamination between the individual laminae. Such damage has been observed to occur even at relatively low impact speeds resulting in a severe loss in the load carrying capacity of the laminae. While the damage is caused by the stresses which develop within the material, the precise nature of these stresses and their relationship to the degree and mode of the damage are not clearly understood at present. This is particularly true in the dynamic case where the stresses are caused by waves whose propagation characteristics are strongly influenced by the inherent anisotropy and heterogeneity of the composite material.

With the increasing use of advanced composites in a variety of modern applications, it has become necessary to employ reliable and effective nondestructive evaluation (NDE) methods to determine the integrity and serviceability of structural composites. Conventional ultrasonic NDE methods, e.g., through-transmission and pulse-echo, based on longitudinal waves, have been effective in detecting relatively large isolated flaws that are parallel to the surfaces of the laminate, but these methods are less useful in detecting and characterizing other common defects, e.g., transverse cracks and partial delamination. The use of ultrasonic experiments consisting of guided waves and contact type transducers have the potential to provide more powerful nondestructive characterization methods for composites. However, the wave phenomena associated with these methods are less well understood than those associated with the conventional techniques and the realization of the full potential of these newer techniques will require a deeper understanding of the wave phenomena than is available at present.

The response of plates to dynamic loads has been studied theoretically by many authors in the past. In much of the early work quasi-static and approximate plate theories have been used[see e.g., Chow (1971); Moon(1973); Sun and Tan (1984); Lal (1984)]. When a composite laminate is subjected to low velocity impact, the generated wavelengths are long compared with its overall dimensions, and the quasistatic and thin plate approximation may be used in stress analysis with useful results. However, for high speed impact as in ultrasonic nondestructive inspection of structural components, the loading rate is several orders of magnitude higher than that for low-velocity impact and the wavelengths are comparable to the thickness of the individual laminae. It is clear that neither quasi-static approximations, nor thin plate theories are adequate in analyzing these problems [Lib and Mal (1995)]. Moreover, there is increasing interest in the use of thicker laminates in a variety of structural applications where the thin plate assumption may not be justified, even for low velocity impact, and where contact type transducers may be needed to increase penetration depth of the waves. A full elastodynamic theory needs to be employed in the solution of the problem in order to obtain accurate estimates of the wave field. Such solutions for the isotropic and quasi-isotropic (*i. e.*, transversely isotropic with symmetry axis normal to the plate surface) cases have also been obtained [e.g. Ceranoglu and Pao (1981), Weaver and Pao (1982), Vasudevan and Mal (1985). The elastodynamic response of a unidirectional composite laminate has been solved by Mal and Lih (1992) and by Liu and Achenbach (1994). To the authors' knowledge, the exact solution of the response of multilayered composite laminates to localized dynamic loads has not appeared in the literature. Although the finite element method has the potential to handle these problems, and a number of codes are currently available [e. g., DYNA3D], the applicability of these codes has

so far been restricted due to the enormous amount of computing effort required in dealing with realistic problems and to the difficulty in giving physical interpretation to the numerical results as well as in accounting for the radiated energy for problems involving propagation in extended media.

In this paper a multitransform technique coupled with the global matrix method developed by Ma] (1988) is used to calculate the displacement and stress fields in a multilayered composite laminate due to a concentrated or distributed dynamic surface load.

11. MATERIAL MODELING

Each lamina in the multilayered composite is modeled as a transversely isotropic and dissipative material (Mal, Bar-Cohen, and Lib, 1992). We assume at the beginning that the time dependence of the field variables is of the form $e^{-i\omega t}$. Solution to problems with arbitrary time dependence can be obtained in a straight forward manner by Fourier inversion of the frequency domain results. In the frequency domain the linear constitutive equation of the transversely isotropic material with its symmetry axis along the x_1 -axis can be expressed in the form

$$\begin{Bmatrix} \sigma_{11} \\ \sigma_{22} \\ \sigma_{33} \\ \sigma_{23} \\ \sigma_{31} \\ \sigma_{12} \end{Bmatrix} = \begin{bmatrix} C_{11} & C_{12} & C_{12} & 0 & 0 & 0 \\ C_{12} & C_{22} & C_{23} & 0 & 0 & 0 \\ C_{12} & C_{23} & C_{22} & 0 & 0 & 0 \\ 0 & 0 & 0 & C_{44} & 0 & 0 \\ 0 & 0 & 0 & 0 & C_{55} & 0 \\ 0 & 0 & 0 & 0 & 0 & C_{55} \end{bmatrix} \begin{Bmatrix} u_{1,1} \\ u_{2,2} \\ u_{3,3} \\ u_{2,3} + u_{3,2} \\ u_{1,3} + u_{3,1} \\ u_{1,2} + u_{2,1} \end{Bmatrix} \quad (1)$$

where $C_{44} = (C_{22} - C_{23})/2$, σ_{ij} is the Cauchy's stress tensor, u_i is the displacement vector and C_{11} , C_{12} , C_{22} , C_{23} , C_{55} are the five independent complex stiffness constants of the material.

Following Mal, Bar-Cohen and Lih (1991), we assume that the complex stiffness constants C_{ij} are related to the real stiffness constants c_{ij} of the material through

$$\begin{aligned} A_1 &= a_1 / (1 + ip\sqrt{a_3/a_1}), \quad A_2 = a_2 / (1 + ip\sqrt{a_3/a_2}), \\ A_3 &= a_3 / (1 + ip\sqrt{a_3/a_3}), \quad A_4 = a_4 / (1 + ip\sqrt{a_3/a_4}), \quad A_5 = a_5 / (1 + ip) \end{aligned} \quad (2)$$

where

$$A_1 = \frac{C_{22}}{\rho}, \quad A_2 = \frac{C_{11}}{\rho}, \quad A_3 = \frac{(C_{12} + C_{55})}{\rho}, \quad A_4 = \frac{C_{44}}{\rho}, \quad A_5 = \frac{C_{55}}{\rho}$$

and a_i is similarly related to c_{ij} . The damping function p is of the form

$$p = p_0 [1 + a_0 (\frac{f}{f_0} - 1)^2 H(f - f_0)] \quad (3)$$

where $\bar{f} = \omega/2\pi$ is the frequency in cycles, $H(f)$ is the Heaviside step function, and p_0 , a_0 , f_0 are constants which determine the degree of decay in the amplitude of the waves with propagation distance. The first term in the right hand side of (3) represents dissipation due to internal friction and other thermodynamic effects, while the second term represents the attenuation caused by wave scattering by the fibers and other inhomogeneities in the material.

III. SOLUTION OF THE DYNAMIC SURFACE LOAD PROBLEM

Consider a multilayered composite laminate of infinite lateral dimensions consisting of N laminae and total thickness H subjected to the surface loading $f(X_1, X_2, t)$ as shown in Fig. 1.

A global coordinate system $X(X_1, X_2, X_3)$ with origin on the top surface of the laminate and an auxiliary local coordinate system $X(x_1, X_2, X_3)$ in each lamina with the x_1 -axis along the fiber direction and x_3 -axis coincident with the global X_3 -axis are introduced. The fiber direction in the m th lamina makes an angle ϕ^m with the X_1 -axis and the thickness of the m th lamina is h^m . The displacement and stress components in the m^* lamina are denoted by u_i^m and σ_{ij}^m in the global coordinate system and by \tilde{u}_i^m and $\tilde{\sigma}_{ij}^m$ in the local coordinate system. Then the displacements and stresses in the local and global coordinate systems are related by

$$\begin{Bmatrix} u_1^m \\ u_2^m \\ u_3^m \end{Bmatrix} = [L^m] \begin{Bmatrix} \tilde{u}_1^m \\ \tilde{u}_2^m \\ \tilde{u}_3^m \end{Bmatrix}, \quad \begin{Bmatrix} \sigma_{31}^m \\ \sigma_{32}^m \\ \sigma_{33}^m \end{Bmatrix} = [L^m] \begin{Bmatrix} \tilde{\sigma}_{31}^m \\ \tilde{\sigma}_{32}^m \\ \tilde{\sigma}_{33}^m \end{Bmatrix}, \quad \begin{Bmatrix} \sigma_{11}^m \\ \sigma_{22}^m \\ \sigma_{12}^m \end{Bmatrix} = [\bar{L}^m] \begin{Bmatrix} \tilde{\sigma}_{11}^m \\ \tilde{\sigma}_{22}^m \\ \tilde{\sigma}_{12}^m \end{Bmatrix}$$

where

$$[L^m] = \begin{bmatrix} c & -s & 0 \\ s & c & 0 \\ 0 & 0 & 1 \end{bmatrix}, \quad [\bar{L}^m] = \begin{bmatrix} c^2 & ss^2 & -2cs \\ s^2 & c^2 & 2cs \\ cs & -cs & c^2 - s^2 \end{bmatrix}$$

and $c = \cos(\phi^m)$, $s = \sin(\phi^m)$. Assuming that $\hat{f}_i(X_1, X_2, \omega)$ is the Fourier time transform of the surface loading $f_i(X_1, X_2, t)$ and denoting the Fourier time transform of the displacement and the stress components $u_i^m(X, t), \sigma_{ij}^m(X, t)$ by $\hat{u}_i^m(X, \omega), \hat{\sigma}_{ij}^m(X, \omega)$, the governing equation becomes

$$\hat{\sigma}_{ij,j}^m + \rho \omega^2 \hat{u}_i^m = 0$$

This equation must be supplemented by the constitutive equation(1) and the solution must satisfy the outgoing wave (or radiation) condition at large lateral distances from the load.

The boundary conditions on the faces of the laminate are

$$\hat{\sigma}_{i3}^1(X_1, X_2, 0, \omega) = -\hat{f}_i(X_1, X_2, \omega) \quad (4a)$$

$$\hat{\sigma}_{i3}^N(X_1, X_2, H, \omega) = 0, \quad i = 1, 2, 3 \quad (4b)$$

Assuming that no delamination occurs at the interfaces, the traction and displacement must be continuous across the interfaces parallel to the X_1 - X_2 plane, i.e.,

$$\begin{aligned} \hat{u}_i^{m-1}(X_1, X_2, X_3^m, \omega) &= \hat{u}_i^m(X_1, X_2, X_3^m, \omega) \\ \hat{\sigma}_{i3}^{m-1}(X_1, X_2, X_3^m, \omega) &= \hat{\sigma}_{i3}^m(X_1, X_2, X_3^m, \omega) \\ i &= 1, 2, 3; m = 2, \dots, N \end{aligned} \quad (5)$$

where X_3^m is the location of the interface between layer m and layer $m-1$. Then under the assumption of initial rest, $\hat{u}_i^m(X, \omega)$, $\hat{\sigma}_{ij}^m(X, \omega)$ can be obtained through the introduction of double spatial Fourier transforms, $\hat{u}_i^m(X, \omega)$, $\hat{\sigma}_{ij}^m(X, \omega)$ and $\hat{f}_i(X_1, X_2, \omega)$ defined by

$$\hat{u}_i^m(X_1, X_2, X_3, \omega) = \frac{1}{4\pi^2} \int_{-\infty}^{\infty} \int_{-\infty}^{\infty} U_i^m(K_1, K_2, X_3, \omega) e^{i(K_1 X_1 + K_2 X_2)} dK_1 dK_2 \quad (6a)$$

$$\hat{\sigma}_{ij}^m(X_1, X_2, X_3, \omega) = \frac{1}{4\pi^2} \int_{-\infty}^{\infty} \int_{-\infty}^{\infty} \Sigma_{ij}^m(K_1, K_2, X_3, \omega) e^{i(K_1 X_1 + K_2 X_2)} dK_1 dK_2 \quad (6b)$$

$$\hat{f}_i(X_1, X_2, \omega) = \frac{1}{4\pi^2} \int_{-\infty}^{\infty} \int_{-\infty}^{\infty} F_i(K_1, K_2, \omega) e^{i(K_1 X_1 + K_2 X_2)} dK_1 dK_2 \quad (6c)$$

where K_1 and K_2 are the global wave numbers in X_1 and X_2 directions, respectively. The details of the solution for the displacement and stress components using the global matrix formulation introduced in Mal (1988) can be found in Lih and Mal (1995). It should be noted that the well known precision problem at high frequencies do not occur in this method [Mal, 1988].

In this paper, we assume that the load is normal to the surface of the laminate and that it can be separated into a time dependent function $f(t)$ and a spatially distributed function $g(X_1, X_2)$; i.e., $f_1 = f_2 = 0$ and $f_3 = f(t)g(X_1, X_2)$. Let the Fourier time transform of $f(t)$ be $\hat{f}(\omega)$, and the spatial double Fourier transform of $g(X_1, X_2)$ be $G(K_1, K_2)$. Then

$$\{F\} = \hat{f}(\omega)\{0, 0, G(K_1, K_2)\} \quad (7)$$

where

$$G(K_1, K_2) = \int_{-\infty}^{\infty} \int_{-\infty}^{\infty} g(X_1, X_2) e^{-i(K_1 X_1 + K_2 X_2)} dX_1 dX_2 \quad (8)$$

For a point load at the origin, $g(x, y) = \delta(x)\delta(y)$, and $G(K_1, K_2) = 1$. For distributed loads, $G(K_1, K_2)$ can be evaluated analytically or numerically. In this paper two types of loads are used in the calculations:

1) Uniform unit load distributed in a rectangular region

Consider a dynamic loading uniformly distributed over a rectangular region $2a \times 2b$ on the surface of the laminate (Fig. 2a). Then the normal force $g(X_1, X_2)$ can be expressed as

$$\begin{aligned} g(X_1, X_2) &= 1, -a < X_1 < a \text{ and } -b < X_2 < b \\ &= 0, \text{ elsewhere} \end{aligned}$$

and

$$G(K_1, K_2) = 4 \int_0^b \int_0^a \cos(K_1 X_1) \cos(K_2 X_2) dX_1 dX_2 = \frac{4 \sin(K_1 a) \sin(K_2 b)}{K_1 K_2}$$

2) Uniform load distributed in a circular region

If the load is uniformly distributed within a circle of radius a (Fig. 2b), then the normal force $g(X_1, X_2)$ can be expressed as

$$g(X_1, X_2) = 1, X_1^2 + X_2^2 \leq a^2 \\ = 0, \text{ elsewhere.}$$

and

$$G(K_1, K_2) = \int_0^a \int_0^{2\pi} e^{iR(K_1 \cos \theta + K_2 \sin \theta)} dR d\theta \\ = \frac{2\pi a J_1(Ka)}{K}, (K \neq 0) \\ \pi a^2, (K = 0)$$

where $K = \sqrt{K_1^2 + K_2^2}$ and $J_1(x)$ is the Bessel function of the first kind of order 1.

3) Gaussian distribution

If the loading is a Gaussian distribution on the surface of the plate (Fig. 2c), then $g(X_1, X_2)$ can be reexpressed in the form

$$g(X_1, X_2) = \frac{P}{s^2} e^{-\frac{X_1^2 + X_2^2}{s^2}}$$

where P is a measure for the strength of the load and s is the standard deviation of the distribution function. With a change of variable to polar coordinates R, θ , $G(K_1, K_2)$ can be expressed as

$$G(K_1, K_2) = Re \frac{C_1}{s^2} \int_0^\infty \int_0^{2\pi} e^{-ikR\cos(\theta) - \frac{R^2}{s^2}} d\theta dR$$

$$= \frac{C_1}{2} \frac{-K^2 s^2}{e^4}$$

where J_0 is the Bessel function of the first kind of order 0. It remains to evaluate the wavenumber integrals in (6) for a suite of frequencies and Fourier inversion using FFT in order to obtain the displacement and stress time histories at a given point in the composite. This is accomplished through the use of an adaptive two-dimensional numerical integration scheme described in Ma] and Lih (1992).

IV. NUMERICAL EXAMPLES

Numerical results for the response of unidirectional and multilayered composite laminates to different types of dynamic surface loads are presented. In all calculations the laminate is assumed to be made up of a AS4/4501 graphite/epoxy composite; its elastic properties are given in Table. 1. The nominal thickness of the laminate is 1 mm. The unit used for force is KN and that for stress is GPa. Approximate results based on the classical plate theory and the shear deformation theory are compared with the exact results, and the range of validity of the approximate solution is determined.

The Force Time History

Three types of pulses are considered in this paper. In order to examine the nature and extent of the numerical] y generated noise before the arrival of the source-generated disturbances at the receiver, a time delay τ_0 was introduced in the source function. This time delay results

Table 1. Material constants of graphite- epoxy composite laminate used in the calculations

Density (g/cm ³)	c ₁₁ (GPa)	c ₁₂	c ₂₂	c ₂₃	c ₅₅	p ₀	f ₀	a ₀
1.578	160.73	6.44	13,92	6,92	7.07	0.005	0.3	0.1

in a phase shift in the frequency domain.

1) A full cycle sine pulse

The sine pulse is useful in developing NDE methods. The function $f(t)$ and its Fourier transform $\hat{f}(\omega)$ can be expressed as

$$\begin{aligned}
 f(t) &= \sin(2\pi t/\tau), \quad 0 < t < \tau \\
 \hat{f}(\omega) &= \frac{\tau i}{\pi} \frac{\sin(\omega \tau/2)}{(1 - \omega \tau/2\pi)} e^{-i\omega \frac{\tau}{2}}, \quad (\omega \neq 2\pi/\tau) \\
 &= \frac{\pi i}{\omega} e^{-i\omega \frac{\tau}{2}}, \quad (\omega = 2\pi/\tau)
 \end{aligned}$$

It can be shown that for $\tau = 1 \mu\text{s}$ the source spectrum vanishes at zero frequency, is maximum at 1 MHz and becomes negligibly small beyond about 5 MHz.

2) A sine-square pulse

This type of source function often arises in impact problems. The function $f(t)$ and its Fourier transform $\hat{f}(\omega)$ can be expressed as

For $\tau = 1 \mu\text{s}$ the source spectrum has a maximum at zero frequency and becomes negligibly small beyond about 3 MHz.

3) A Gaussian Pulse

$$f(t) = \sin^2(\pi t/\tau), \quad 0 < t < \tau$$

$$\hat{f}(\omega) = \frac{i}{2\omega} \frac{e^{-i\omega\tau/2} - 1}{[1 - (\omega\tau/2\pi)^2]} \quad (\omega \neq 2\pi/\tau)$$

$$-\tau/4, \quad (\omega = 2\pi/\tau)$$

The function $f(t)$ and its Fourier transform $\hat{f}(\omega)$ can be expressed as

$$f(t) = \frac{1}{\sqrt{2\pi}\sigma} e^{-\frac{t^2}{2\sigma^2}} \quad -\infty < t < \infty$$

$$\hat{f}(\omega) = \frac{1}{\sigma^2} e^{-\frac{\omega^2\sigma^2}{2}}$$

For $\sigma = 1 \mu\text{s}$ the source spectrum has a maximum at zero frequency and becomes negligibly small beyond about 1 MHz.

Typical frequency domain results for the kernel $U_3(K_1, O)$ in a 1 mm $[0,90]$, composite laminate at 0.5 MHz frequency are shown in Fig. 4 for the exact solution, shear deformation plate approximation, and the classical plate approximation. It is obvious that the approximate solutions are inaccurate as was previously found in Lih and Mal (1995). The time history of the stress component σ_{11} for the distributed load in a circle with the sine square pulse shape for a unidirectional composite at different locations on its top surface is shown in Fig. 5. The case of the concentrated load with the full cycle sine pulse is shown in Fig. 6. It can be seen that in both Figs. 5 and 6 the stress waves travel faster along 0° , and that the point source produces higher frequency oscillations in the stresses.

The results for multilayered laminates are shown in Figs. 7 through 11. In these figures ϕ refers to the angle of propagation of the waves to the fibers in the top lamina. Fig. 7 shows the time history of the normal displacement on the top surface of a quasi-isotropic $[0, \pm 45, 90]$,

laminate subjected to the Gaussian distributed load with the full cycle sine pulse for $t_0 = 0$ and $T = 0.5 \mu s$. It can be seen that the main pulse in the surface motion is the flexural wave and the high frequency oscillations appear after the main pulse. The spectra of the time histories are plotted in Fig. 8. The peaks in the spectra are associated with the high frequency oscillations of the time histories and they occur at frequencies corresponding to the first cut-off of the higher mode in the dispersion curves (c. f. Mal, Yin, and Bar-Cohen, 1991). The time history and spectra of σ_{33} at the first interface ($X_3 = 0.125$ mm) in the quasi-isotropic laminate subjected to the load on the square area with full cycle sine pulse are shown in Fig. 9 for $t_0 = 0$ and $\tau = 1 \mu s$. It can be seen that the time history of σ_{33} consists of a pulse equal to the negative of the source followed by highly oscillatory waves. The maximum stress at a distance of 5 mm from the origin is about 20% of the traction at the source. Furthermore, the frequency of the oscillation is higher for field points close to 0° and 90° and decays out faster at 45° . The calculation of σ_{33} can be used to predict the delamination between the lamina. Fig. 10 shows the spectra of Fig. 9. As in Fig. 8, the main distinguishing feature of the spectra is the peak at the cutoff frequencies. Fig. 11 shows the time history and spectra of σ_{33} at the interfaces, $X_3 = 0.25$ mm and 0.75 mm, in a $[0, 90]_s$ laminate subjected to a concentrated load and the full cycle sine pulse for $t_0 = 0$ and $\tau = 1 \mu s$. It can be seen that the bottom interface under the source is subjected to strong tensile stresses even though the loading at the top is compression, which may cause delamination at this interface.

V. CONCLUDING REMARKS

The elastodynamic field produced in unidirectional and multilayered composite laminates due to localized dynamic surface loads have been studied in this paper. The proposed multiple transform technique appears to work well and is able to calculate the displacements and stresses for concentrated as well as distributed surface loads of arbitrary time dependence. Although the associated numerical codes are CPU-intensive, they are much more efficient than other available codes for the analysis of three-dimensional models of the composite laminate. The method is expected to be useful for the prediction of failure modes of structural composites. The method can also be used in developing NDE methods for the prediction of the waveforms produced by point source triggers with contact type of transducers. Future work should involve parameter studies for different stacking sequences of the lamina and various types of sources.

ACKNOWLEDGEMENT

This research was supported by AFOSR under grant F49620-93-1 -0320 monitored by Dr. Walter Jones.

REFERENCES

- Abrate, S. (1991). "Impact on Laminated Composite Materials", *Appl. Mech Rev* **44**, 155-190.
- Bar-Cohen, Y. (1987). "Ultrasonic NDE of Composite - a Review", in *Solid Mechanics Research for Quantitative NDE* (Edited by J.D. Achenbach and Y. Rajapakse), pp. 197 -201. Marinus Nijhoff, Boston.
- Ceranoglu A. N., and Pao, Y. H. (1981). "Propagation of Elastic Pulses and Acoustic Emission in a Plate", *ASME J. Appl. Mech.* **48**, 125-147.
- La], K. M. (1984). "Coefficients of Restitution for Low Velocity Transverse Impact on Thin Graphite-Epoxy Laminates", *Composite Technology Review* **6**, 112-117.
- Lib, S., and Mal, A. K. (1995). "On the Accuracy of Approximate Plate Theories for Wave Field Calculations in Theories for Wave Field Calculations in Composite Laminates", *Wave Motion* (in press).
- Liu, G. R., Tani, J., Ohyoshi, T. and Watanabe, K. (1991a). "Transient Waves in Anisotropic Laminated Plates", Part 1 &2, *J. of Vibration and Acoustics* **113**, 230-239.
- Liu, G. R., Tani, J., Ohyoshi, T. and Watanabe, K. (1991a). "Characteristic Wave Surfaces in Anisotropic Laminated Plates", *J. of Vibration and Acoustics* **113**, 279-285.
- Liu, G. R. and Achenbach, J. D. (1994). "A Strip Element Method for Stress Analysis of Anisotropic Linearly Elastic Solids," *J. Appl. Mech.* **61**, 270 -277.
- Mal, A. K. (1988). "Wave Propagation in Layered Composite Laminates Under Periodic Surface Loads", *Wave Motion* **10**, 257-266.
- Mal, A. K., Yin, C.-C., and Bar-Cohen, Y. (1991), "Ultrasonic Nondestructive Evaluation of Cracked Composite Laminates", *Composites Engineering* **1**, 85-101.
- Mal, A. K., and Yin, C. -C. and Bar-Cohen, Y. (1992). "Analysis of Acoustic pulses Reflected from the fiber-Reinforced Composite Laminates", *J. Appl. Mech* **59**, 5136-5144.
- Mal, A. K., and Lib, S.-S. (1992). "Elastodynamic Response of a Unidirectional Composite Laminate to Concentrated Surface Loads, Parts I, II", *ASME J. Appl. Mech.* **55**, 878-892.
- Mal, A. K., Bar-Cohen, Y. and Lib, S.-S. (1992). "Wave Attenuation in Fiber-Reinforced Composites", *International Symposium on Mechanics and Mechanisms of Material Damping (M³D)*, ASTM STP 1169, 245-261.

Sun, C. T. and Tan, T. M. (1984). "Wave Propagation in a Graphite/Epoxy Laminate", *J. Astro. Sci.* 32, 269-284.

Weaver, R. L., and Pao, Y. H. (1982). "Axisymmetric Elastic Waves Excited by a Point Source in a Plate", *ASME J. Appl. Mech.* 49, 821-836.

Wu, H.-Y. T. and Springer, G. S. (1988). "Measurements of Matrix Cracking and Delamination Caused by Impact on Composite Plates", *J. Composite Materials* 22, 518-532.

Vasudevan, N., and Mal, A. K. (1985). "Response of an Elastic Plate to Localized Transient Sources", *J. of Appl. Mech.* 52, 356-362.

Figure Captions:

Fig. 1. Geometry of the composite laminate.

Fig. 2. Surface load: (a) in a rectangular area (b) in a circular area (c) Gaussian distribution.

Fig. 3. Time history and spectrum of source function for (a) a full cycle of sin pulse (b) a full cycle of sin-square pulse (c) a Gaussian.

Fig. 4. Behavior of the kernel U_3 for a 1 mm $[0,90]_s$ composite laminate at frequency = 0.5 MHz.

Fig. 5. The time history of the stress σ_{11} in a 1 mm unidirectional composite laminate subjected to a uniform distributed surface load on a 1 mm radius circular region, with a sine square pulse for $t_0 = 5$ and $\tau = 1 \mu s$.

Fig. 6. The time history of the stress σ_{11} in a 1 mm unidirectional composite laminate subject to a point load with a sine pulse for $t_0 = 5$ and $\tau = 1 \mu s$.

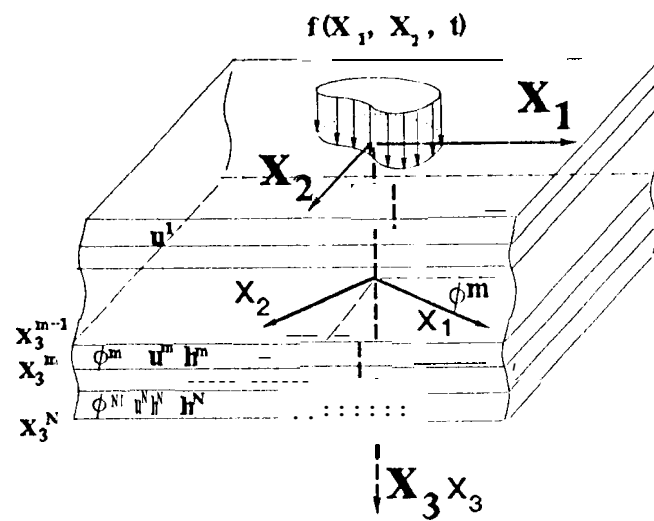
Fig. 7. The time history of the displacement u_3 in a 1 mm $[0, *45, 90]_s$ composite laminate subjected to a Gaussian distributed surface load with a sine pulse for $t_0 = 0$ and $\tau = 1 \mu s$.

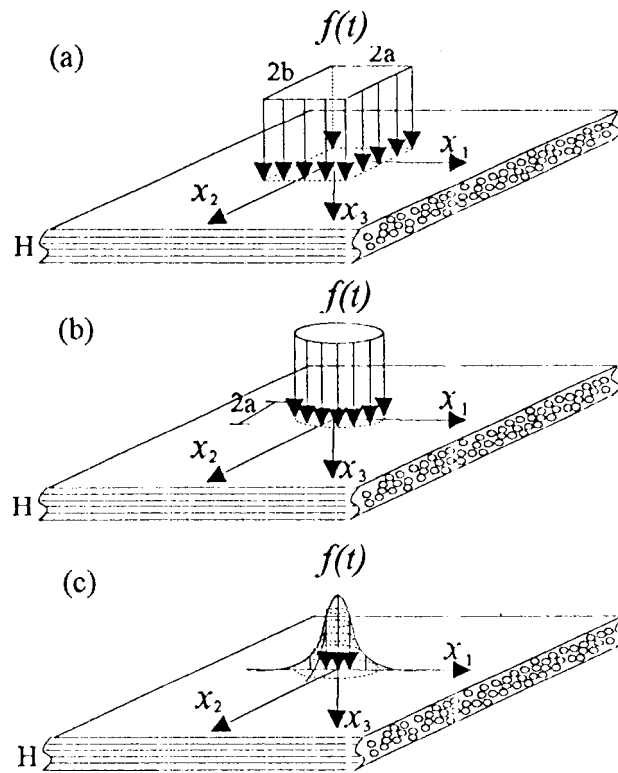
Fig. 8. Spectra of Fig. 7.

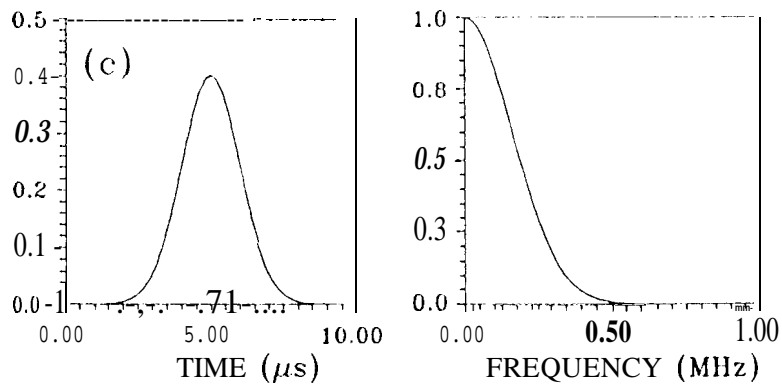
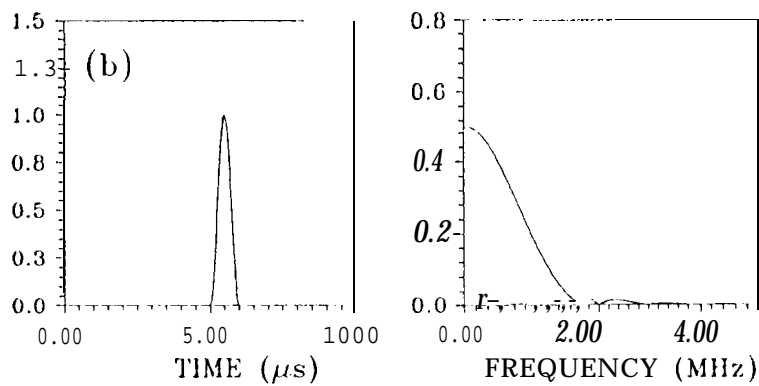
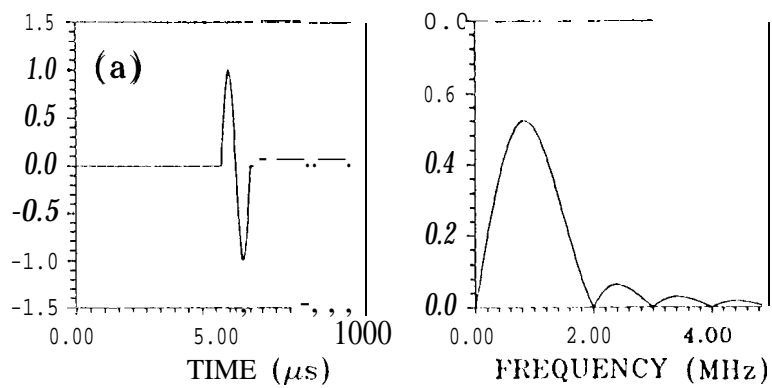
Fig. 9. The time history of the stress σ_{33} in a 1 mm $[0, \pm 45, 90]_s$ composite laminate subjected to a uniform distributed surface load on a $2 \times 2 \text{ mm}^2$ square with a sine pulse for $t_0 = 0$ and $\tau = 1 \mu s$.

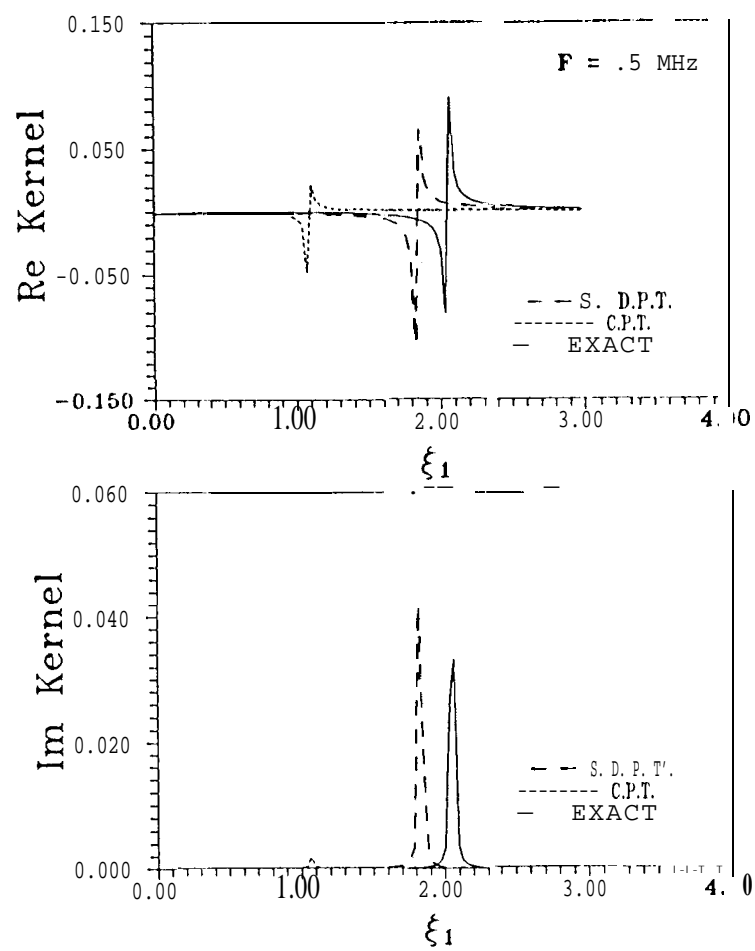
Fig. 10. Spectra of Fig. 9.

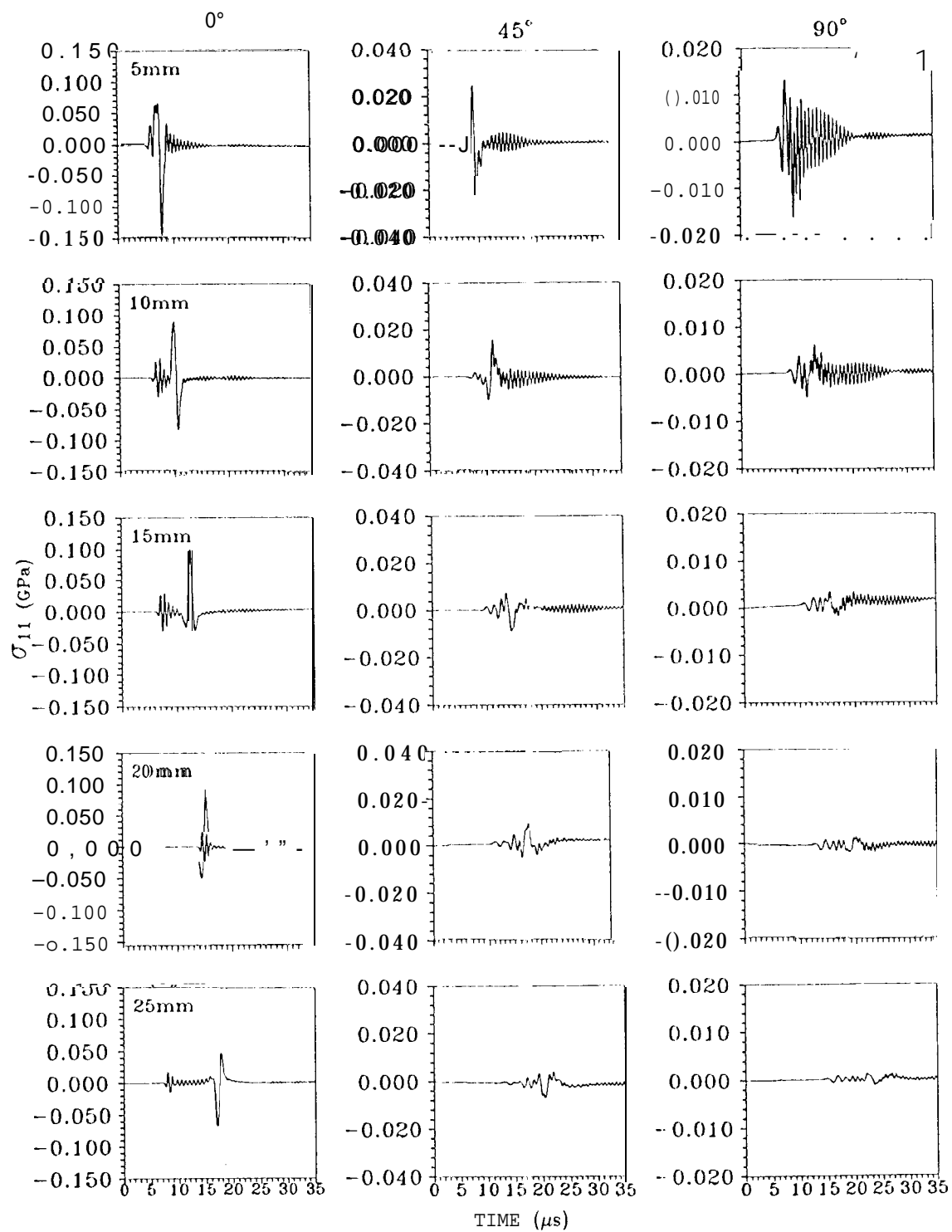
Fig. 11. The time history of the stress σ_{33} in a 1 mm $[0, 90]_s$ composite laminate subjected to a concentrated surface load with a sine square pulse for $t_0 = 0$ and $\tau = 1 \mu s$.





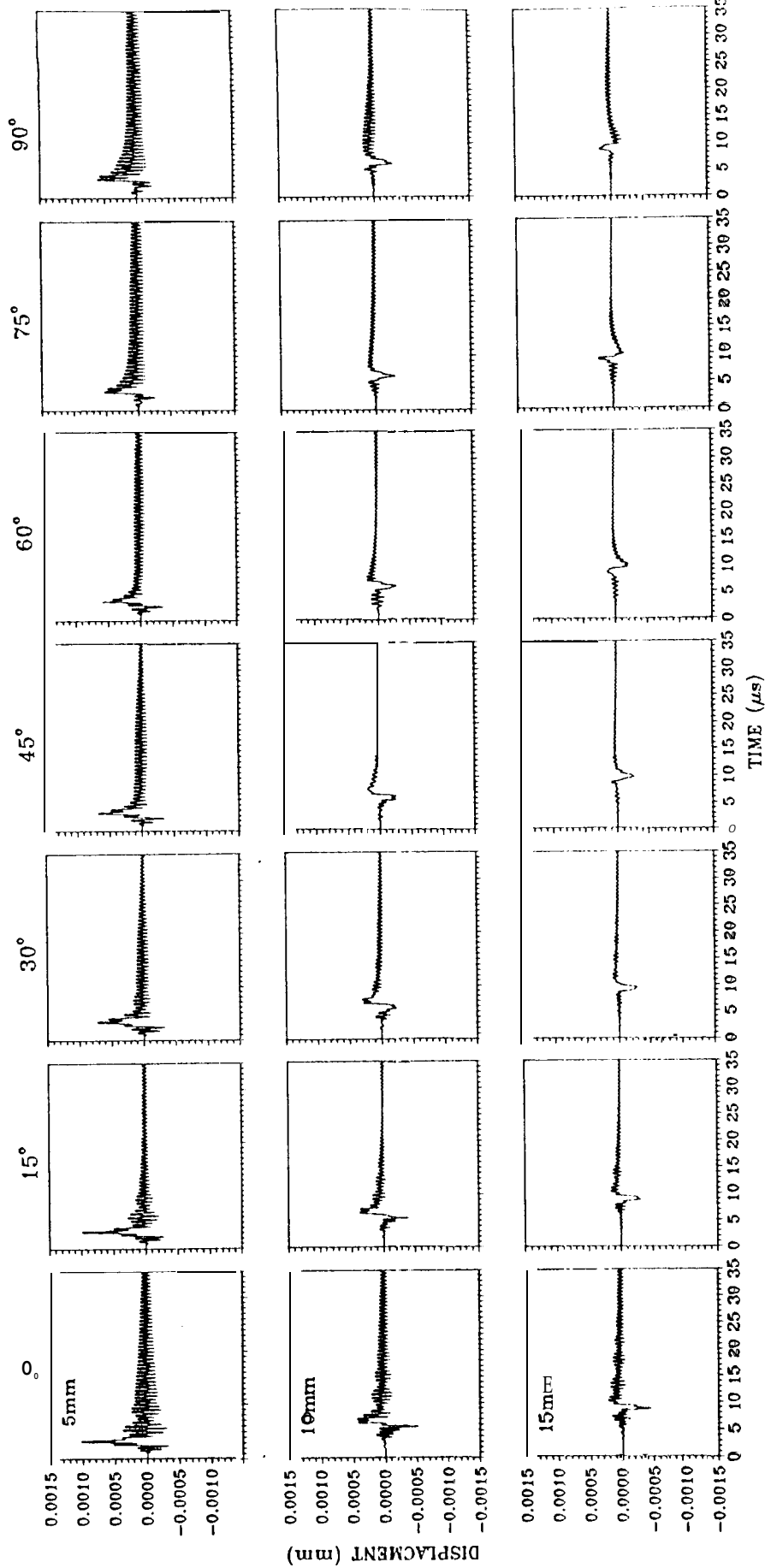


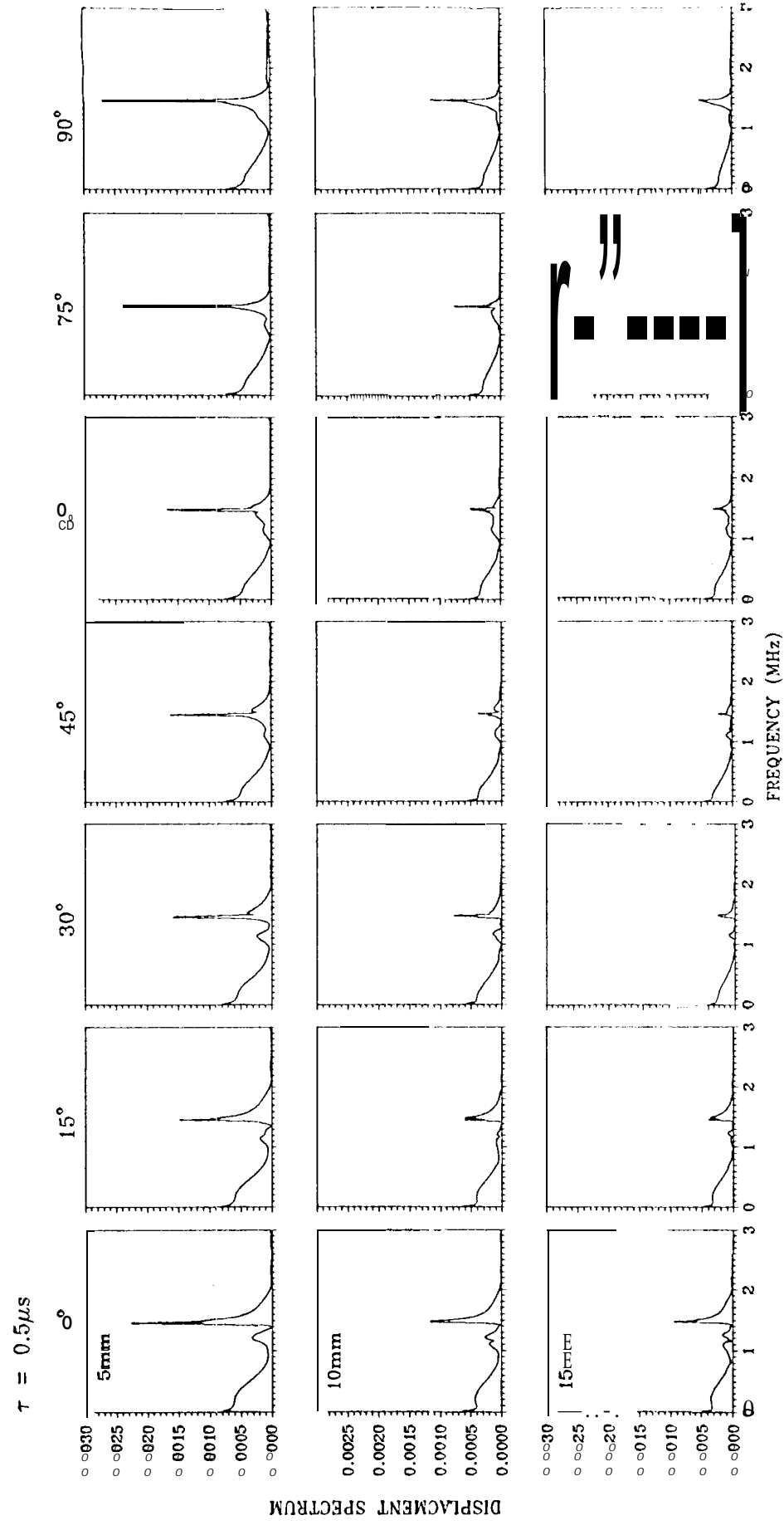




FL

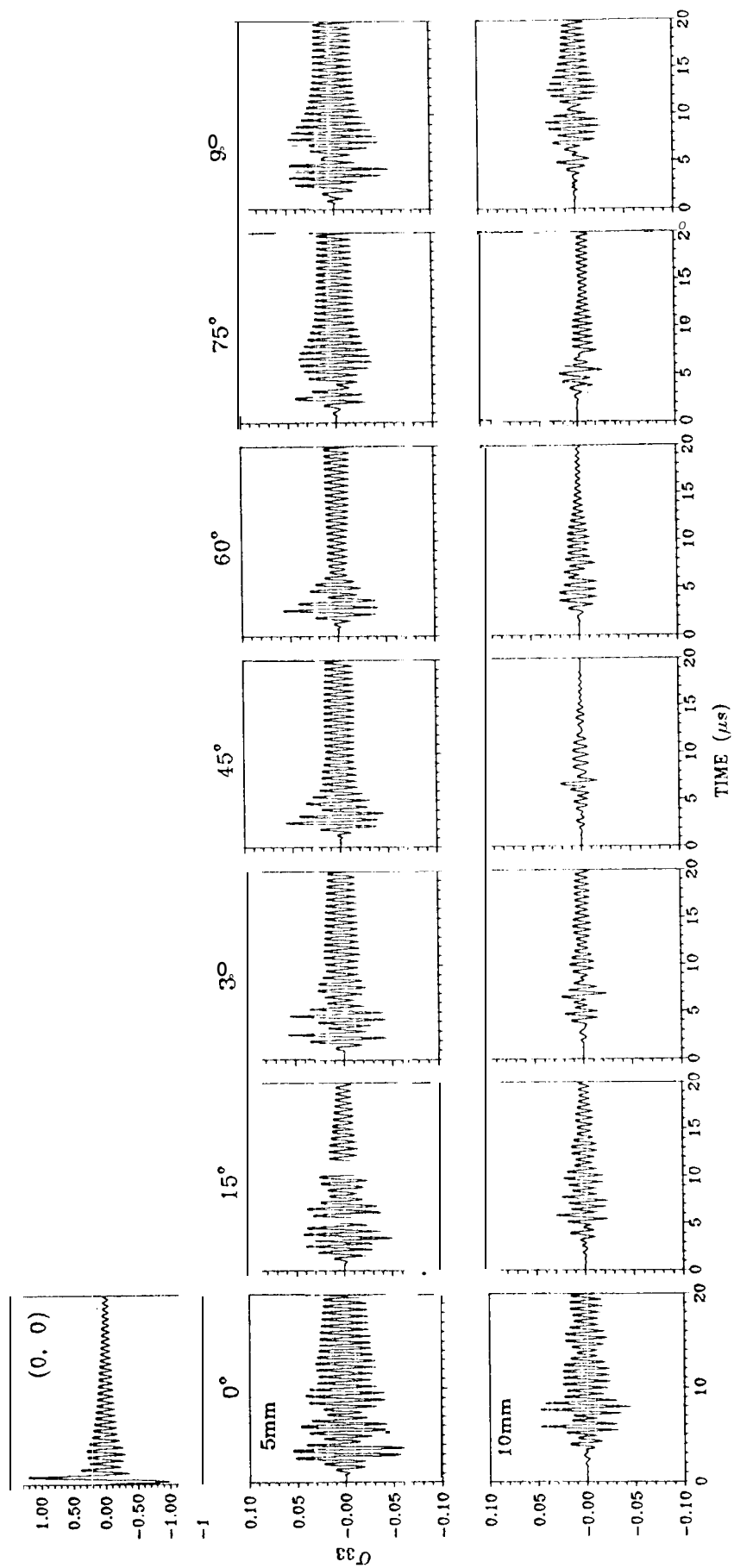
$\tau = 0.5 \mu s$





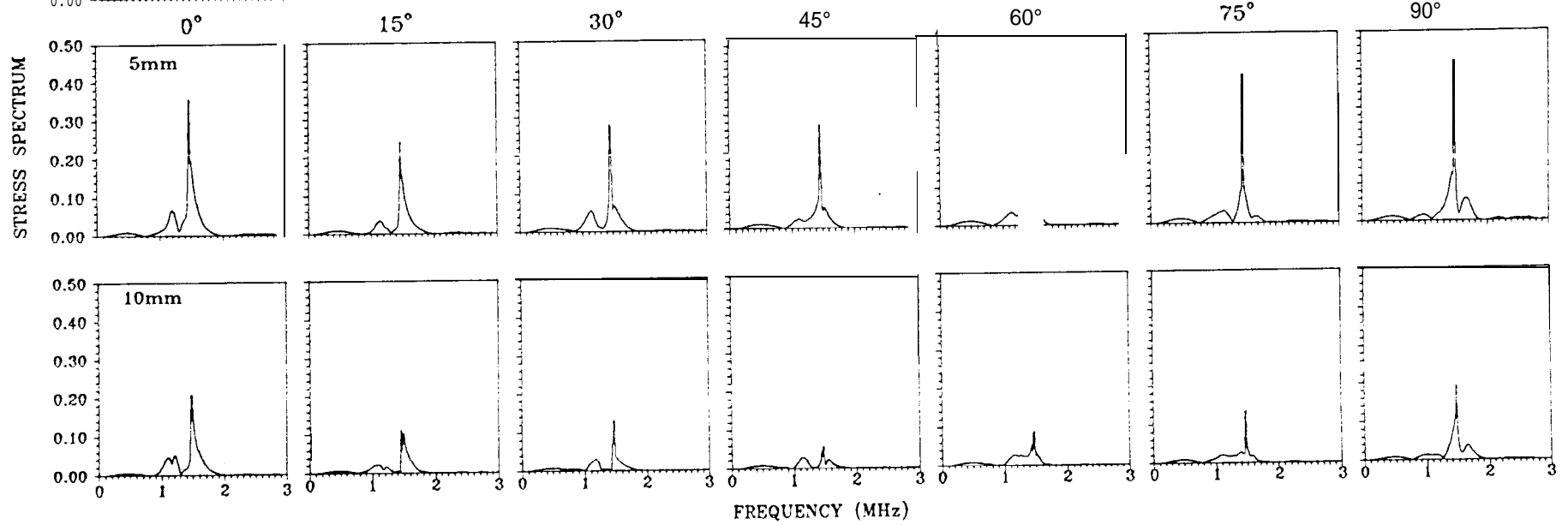
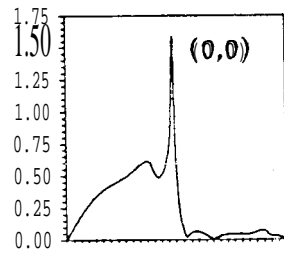
$\tau = 1 \mu s$

$X_3 = 0.25$

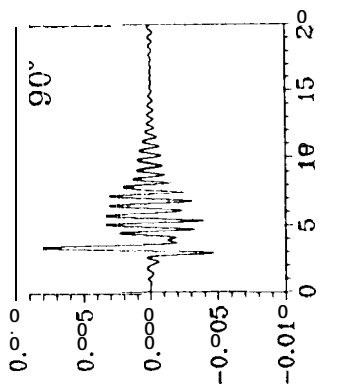
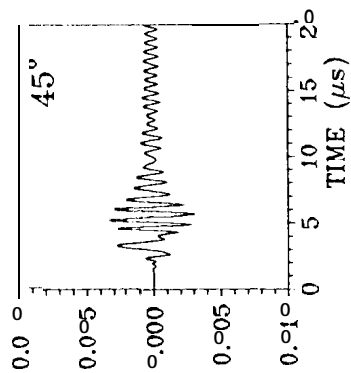
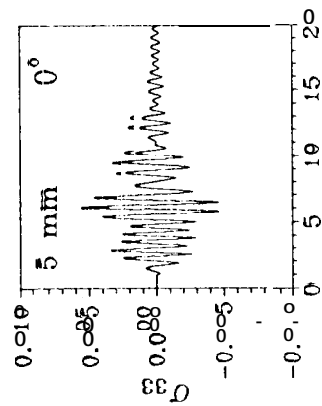
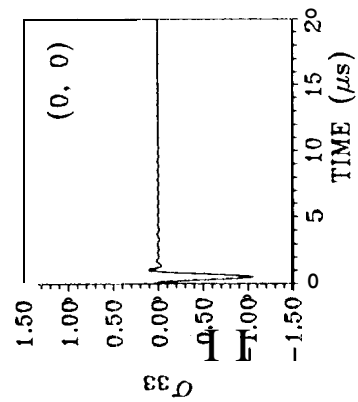


$$\tau = 1 \mu s$$

$$x_3 = 0.125 \text{ mm}$$



$X_3 = .25 \text{ mm}$



$X_3 = .75 \text{ mm}$

